

1  
2  
3  
4  
5  
6  
7  
8  
9  
10  
11  
12  
13  
14  
15  
16  
17  
18  
19  
20  
21  
22  
23  
24  
25  
26  
27  
28  
29  
30  
31  
32  
33  
34  
35  
36  
37  
38  
39  
40  
41  
42  
43  
44  
45  
46  
47  
48  
49  
50  
51  
52  
53  
54  
55  
56  
57  
58  
59  
60  
61  
62  
63  
64  
65

# Neural Network-derived perfusion maps: a Model-free approach to computed tomography perfusion in patients with acute ischemic stroke

Umberto A. Gava<sup>a,b</sup>, Federico D'Agata<sup>b</sup>, Enzo Tartaglione<sup>c</sup>, Marco Grangetto<sup>c</sup>, Francesca Bertolino<sup>a,b</sup>, Ambra Santonocito<sup>b</sup>, Edwin Bennink<sup>d,e</sup>, Mauro Bergui<sup>a,b</sup>

<sup>a</sup>Neuroradiology Division Molinette Hospital, Turin (Italy); <sup>b</sup> Neuroscience Department, University of Turin (Italy); <sup>c</sup> Informatics Department, University of Turin, Turin (Italy); <sup>d</sup> Department of Radiology, University Medical Center Utrecht, Utrecht, the Netherlands; <sup>e</sup> Image Sciences Institute, University Medical Center Utrecht, Utrecht, the Netherlands.

Corresponding Author: Address correspondence to Umberto A. Gava,  
Neuroradiology division, Molinette Hospital, Turin (TO), Corso Bramante 88/90,  
10126. E-mail: [umbertogava@gmail.com](mailto:umbertogava@gmail.com)

Federico D'Agata ([federico.dagata@unito.it](mailto:federico.dagata@unito.it)), Enzo Tartaglione ([enzo.tartaglione@unito.it](mailto:enzo.tartaglione@unito.it)),  
Marco Grangetto ([marco.grangetto@unito.it](mailto:marco.grangetto@unito.it)), Francesca Bertolino  
([francesca.bertolino@unito.it](mailto:francesca.bertolino@unito.it)), Ambra Santonocito ([ambra.santonocito@unito.it](mailto:ambra.santonocito@unito.it)), Edwin  
Bennink ([H.E.Bennink-2@umcutrecht.nl](mailto:H.E.Bennink-2@umcutrecht.nl)), Mauro Bergui ([mauro.bergui@unito.it](mailto:mauro.bergui@unito.it))

**NOTE: This preprint reports new research that has not been certified by peer review and should not be used to guide clinical practice.**

## Abstract

1  
2  
3  
4  
5  
6 Purpose: In this study we investigate whether a Convolutional Neural Network (CNN)  
7  
8 can generate clinically relevant parametric maps from CT perfusion data in a clinical  
9  
10 setting of patients with acute ischemic stroke.

11  
12  
13 Methods: Training of the CNN was done on a subset of 100 perfusion data, while 15  
14  
15 samples were used as validation. All the data used for the training/validation of the  
16  
17 network and to generate ground truth (GT) maps, using a state-of-the-art  
18  
19 deconvolution-algorithm, were previously pre-processed using a standard pipeline.

20  
21  
22 Validation was carried out through manual segmentation of infarct core and  
23  
24 penumbra on both CNN-derived maps and GT maps. Concordance among  
25  
26 segmented lesions was assessed using the Dice and the Pearson correlation  
27  
28 coefficients across lesion volumes.

29  
30  
31 Results: Mean Dice scores from two different raters and the GT maps were > 0.70  
32  
33 (good-matching). Inter-rater concordance was also high and strong correlation was  
34  
35 found between lesion volumes of CNN maps and GT maps (0.99, 0.98).

36  
37  
38 Conclusion: Our CNN-based approach generated clinically relevant perfusion maps  
39  
40 that are comparable to state-of-the-art perfusion analysis methods based on  
41  
42 deconvolution of the data. Moreover, the proposed technique requires less  
43  
44 information to estimate the ischemic core and thus might allow the development of  
45  
46 novel perfusion protocols with lower radiation dose.

47  
48  
49  
50  
51  
52  
53  
54  
55 Keywords: CNN; CT-perfusion; maps; stroke

56  
57  
58  
59  
60  
61  
62  
63  
64  
65  
66  
67  
68  
69  
70  
71  
72  
73  
74  
75  
76  
77  
78  
79  
80  
81  
82  
83  
84  
85  
86  
87  
88  
89  
90  
91  
92  
93  
94  
95  
96  
97  
98  
99  
100  
101  
102  
103  
104  
105  
106  
107  
108  
109  
110  
111  
112  
113  
114  
115  
116  
117  
118  
119  
120  
121  
122  
123  
124  
125  
126  
127  
128  
129  
130  
131  
132  
133  
134  
135  
136  
137  
138  
139  
140  
141  
142  
143  
144  
145  
146  
147  
148  
149  
150  
151  
152  
153  
154  
155  
156  
157  
158  
159  
160  
161  
162  
163  
164  
165  
166  
167  
168  
169  
170  
171  
172  
173  
174  
175  
176  
177  
178  
179  
180  
181  
182  
183  
184  
185  
186  
187  
188  
189  
190  
191  
192  
193  
194  
195  
196  
197  
198  
199  
200  
201  
202  
203  
204  
205  
206  
207  
208  
209  
210  
211  
212  
213  
214  
215  
216  
217  
218  
219  
220  
221  
222  
223  
224  
225  
226  
227  
228  
229  
230  
231  
232  
233  
234  
235  
236  
237  
238  
239  
240  
241  
242  
243  
244  
245  
246  
247  
248  
249  
250  
251  
252  
253  
254  
255  
256  
257  
258  
259  
260  
261  
262  
263  
264  
265  
266  
267  
268  
269  
270  
271  
272  
273  
274  
275  
276  
277  
278  
279  
280  
281  
282  
283  
284  
285  
286  
287  
288  
289  
290  
291  
292  
293  
294  
295  
296  
297  
298  
299  
300  
301  
302  
303  
304  
305  
306  
307  
308  
309  
310  
311  
312  
313  
314  
315  
316  
317  
318  
319  
320  
321  
322  
323  
324  
325  
326  
327  
328  
329  
330  
331  
332  
333  
334  
335  
336  
337  
338  
339  
340  
341  
342  
343  
344  
345  
346  
347  
348  
349  
350  
351  
352  
353  
354  
355  
356  
357  
358  
359  
360  
361  
362  
363  
364  
365  
366  
367  
368  
369  
370  
371  
372  
373  
374  
375  
376  
377  
378  
379  
380  
381  
382  
383  
384  
385  
386  
387  
388  
389  
390  
391  
392  
393  
394  
395  
396  
397  
398  
399  
400  
401  
402  
403  
404  
405  
406  
407  
408  
409  
410  
411  
412  
413  
414  
415  
416  
417  
418  
419  
420  
421  
422  
423  
424  
425  
426  
427  
428  
429  
430  
431  
432  
433  
434  
435  
436  
437  
438  
439  
440  
441  
442  
443  
444  
445  
446  
447  
448  
449  
450  
451  
452  
453  
454  
455  
456  
457  
458  
459  
460  
461  
462  
463  
464  
465  
466  
467  
468  
469  
470  
471  
472  
473  
474  
475  
476  
477  
478  
479  
480  
481  
482  
483  
484  
485  
486  
487  
488  
489  
490  
491  
492  
493  
494  
495  
496  
497  
498  
499  
500  
501  
502  
503  
504  
505  
506  
507  
508  
509  
510  
511  
512  
513  
514  
515  
516  
517  
518  
519  
520  
521  
522  
523  
524  
525  
526  
527  
528  
529  
530  
531  
532  
533  
534  
535  
536  
537  
538  
539  
540  
541  
542  
543  
544  
545  
546  
547  
548  
549  
550  
551  
552  
553  
554  
555  
556  
557  
558  
559  
560  
561  
562  
563  
564  
565  
566  
567  
568  
569  
570  
571  
572  
573  
574  
575  
576  
577  
578  
579  
580  
581  
582  
583  
584  
585  
586  
587  
588  
589  
590  
591  
592  
593  
594  
595  
596  
597  
598  
599  
600  
601  
602  
603  
604  
605  
606  
607  
608  
609  
610  
611  
612  
613  
614  
615  
616  
617  
618  
619  
620  
621  
622  
623  
624  
625  
626  
627  
628  
629  
630  
631  
632  
633  
634  
635  
636  
637  
638  
639  
640  
641  
642  
643  
644  
645  
646  
647  
648  
649  
650  
651  
652  
653  
654  
655  
656  
657  
658  
659  
660  
661  
662  
663  
664  
665  
666  
667  
668  
669  
670  
671  
672  
673  
674  
675  
676  
677  
678  
679  
680  
681  
682  
683  
684  
685  
686  
687  
688  
689  
690  
691  
692  
693  
694  
695  
696  
697  
698  
699  
700  
701  
702  
703  
704  
705  
706  
707  
708  
709  
710  
711  
712  
713  
714  
715  
716  
717  
718  
719  
720  
721  
722  
723  
724  
725  
726  
727  
728  
729  
730  
731  
732  
733  
734  
735  
736  
737  
738  
739  
740  
741  
742  
743  
744  
745  
746  
747  
748  
749  
750  
751  
752  
753  
754  
755  
756  
757  
758  
759  
760  
761  
762  
763  
764  
765  
766  
767  
768  
769  
770  
771  
772  
773  
774  
775  
776  
777  
778  
779  
780  
781  
782  
783  
784  
785  
786  
787  
788  
789  
790  
791  
792  
793  
794  
795  
796  
797  
798  
799  
800  
801  
802  
803  
804  
805  
806  
807  
808  
809  
810  
811  
812  
813  
814  
815  
816  
817  
818  
819  
820  
821  
822  
823  
824  
825  
826  
827  
828  
829  
830  
831  
832  
833  
834  
835  
836  
837  
838  
839  
840  
841  
842  
843  
844  
845  
846  
847  
848  
849  
850  
851  
852  
853  
854  
855  
856  
857  
858  
859  
860  
861  
862  
863  
864  
865  
866  
867  
868  
869  
870  
871  
872  
873  
874  
875  
876  
877  
878  
879  
880  
881  
882  
883  
884  
885  
886  
887  
888  
889  
890  
891  
892  
893  
894  
895  
896  
897  
898  
899  
900  
901  
902  
903  
904  
905  
906  
907  
908  
909  
910  
911  
912  
913  
914  
915  
916  
917  
918  
919  
920  
921  
922  
923  
924  
925  
926  
927  
928  
929  
930  
931  
932  
933  
934  
935  
936  
937  
938  
939  
940  
941  
942  
943  
944  
945  
946  
947  
948  
949  
950  
951  
952  
953  
954  
955  
956  
957  
958  
959  
960  
961  
962  
963  
964  
965  
966  
967  
968  
969  
970  
971  
972  
973  
974  
975  
976  
977  
978  
979  
980  
981  
982  
983  
984  
985  
986  
987  
988  
989  
990  
991  
992  
993  
994  
995  
996  
997  
998  
999  
1000

- Convolutional Neural Network (CNN),
- Cerebral Blood Volume (CBV),
- Cerebral Blood Flow (CBF),
- Time to Peak (TTP),
- CT Perfusion (CTP),
- CT Angiography (CTA),
- Acute ischemic Stroke (AIS),
- Arterial Input Function (AIF),
- Venous Output Function (VOF),
- Impulse Response Function (IRF).

1  
2  
3  
4  
5  
6  
7  
8  
9  
10  
11  
12  
13  
14  
15  
16  
17  
18  
19  
20  
21  
22  
23  
24  
25  
26  
27  
28  
29  
30  
31  
32  
33  
34  
35  
36  
37  
38  
39  
40  
41  
42  
43  
44  
45  
46  
47  
48  
49  
50  
51  
52  
53  
54  
55  
56  
57  
58  
59  
60  
61  
62  
63  
64  
65

# 1. Introduction

Occlusion of a cerebral artery causes sudden decrease of the blood perfusion in the vascular territory matching the occluded vessel. The peripheral regions of the area affected by the vascular occlusion have their blood flow deficit reduced by the collateral circulation, in comparison to the centre of the affected territory. In fact, ischemic lesions develop rapidly, originating from the centre of the occluded vascular territory and progressively expanding to the most peripheral regions.

From the onset of symptoms, in the ischemic non-functioning area of the brain two different regions may be identified: a central “core”, and a peripheral “penumbra”, respectively corresponding to areas of irreversible damage and potential recovery, provided recanalization of the occluded vessel. Therefore, identification of core and penumbra may predict the fate of the tissue and drive reperfusion treatments.[1,2]

The extension of core and penumbra may be estimated clinically, from the symptoms and their onset time, or using perfusion techniques, in particular CT Perfusion (CTP).

During CTP, a series of low-dose scans are acquired after contrast bolus injection, allowing to compute time-density curves; deconvolution of these curves allows for generating parametric maps to track perfusion parameters dynamics. Cerebral Blood Volume (CBV), Cerebral Blood Flow (CBF), time to peak (TTP) and mean transit time (MTT) are the estimated perfusion parameters most frequently used in clinical practice. CBV is considered a marker of core, while CBF, TTP, MTT mark penumbra.[3–5]

The role of CTP is particularly critical in patients with unknown time from onset, or out of the 4.5 and 6 hours windows used to select patients for intra-venous and intra-

1 arterial reperfusion treatments, respectively. Two trials (DAWN and DEFUSE)  
2 demonstrated clinical usefulness of intra-arterial reperfusion in patients selected  
3 using CBV and CBF estimation based on CTP.[6,7]  
4  
5  
6  
7

8  
9 Different algorithms are used to perform deconvolution of time-intensity curves,  
10 some of which are not public and may produce largely different maps.[8] In an ideal  
11 setting of limited noise, limited variance and no movement artefact, a pixel-by-pixel  
12 analysis, as performed by deconvolution-based algorithms, is probably the best  
13 choice to obtain realistic, affordable and reproducible maps. Unfortunately, in the real  
14 world, information has to be kept redundant in order to overcome problems due to  
15 noise, large variances and movement artefacts. In practice, this imposes to obtain  
16 more slices, requiring a larger number of acquisitions and more X-ray exposure for  
17 the patients, the extraction of an arterial input function (AIF), and a series of spatial  
18 pre-processing steps for noise and variance reduction.  
19  
20  
21  
22  
23  
24  
25  
26  
27  
28  
29  
30  
31  
32  
33

34 Luckily, employing Machine Learning approaches to the problem of deconvolving  
35 time-intensity curves, offers several potential advantages over canonical algorithms,  
36 allowing the extraction of information that is relatively insensitive to noise,  
37 misalignments and variance.  
38  
39  
40  
41  
42  
43

44 In our study we want to explore whether a properly trained Convolutional Neural  
45 Network (CNN), based on a U-Net-like structure, can generate clinically relevant  
46 parametric maps of CBV, CBF and time to peak TTP on a pre-processed dataset of  
47 CTP images. CTP images were obtained from a real-world dataset of patients with  
48 acute ischemic stroke (AIS), no large lesions on non-contrast CT scan, and  
49 candidates for reperfusion therapies.[9] This dataset was chosen because it  
50  
51  
52  
53  
54  
55  
56  
57  
58  
59  
60  
61  
62  
63  
64  
65

1  
2  
3  
4  
5  
6  
7  
8  
9  
10  
11  
12  
13  
14  
15  
16  
17  
18  
19  
20  
21  
22  
23  
24  
25  
26  
27  
28  
29  
30  
31  
32  
33  
34  
35  
36  
37  
38  
39  
40  
41  
42  
43  
44  
45  
46  
47  
48  
49  
50  
51  
52  
53  
54  
55  
56  
57  
58  
59  
60  
61  
62  
63  
64  
65

corresponds to the one used in the DAWN and DEFUSE trials, for which perfusion studies drive reperfusion therapies.

## 2. Materials and Methods

### 2.1 Clinical Data

Perfusion data from 127 consecutive patients were retrospectively obtained from hospital PACS. 12 of them, with unreliable data, were discharged (no contrast seen, excess of movements premature termination of acquisition). The remaining 115 datasets were randomly split into a subset of 100, to train the CNN, and 15, to validate results.

CTP acquisition parameters were as follows: Scanner GE 64 slice, 80 kV, 150 mAs, 44.5 sec duration, 89 volumes (40 mm axial coverage), injection of 40 ml of Iodine contrast agent (300 mg/ml) at 4 ml/s speed.

### 2.2 Calculation of ground truth maps

1  
2 We calculated perfusion maps, including CBF, CBV, TTP, using a standard pipeline  
3  
4 of spatial pre-processing and a state-of-the-art fast model-based non-linear  
5  
6 regression (NLR) method developed By Bennink e al.[10]  
7

8  
9 Motion correction was done using a rigid registration method and subsequently all  
10  
11 images were filtered implementing a bilateral filter.[11,12]  
12  
13

14 AIF and Venous output function (VOF) calculation was done automatically on a 100  
15  
16 voxels sample.  
17

18  
19 The box-shaped model developed by Bennink et al. describes the impulse response  
20  
21 function (IRF) of the perfused tissue in terms of CBV, MTT and tracer delay. The  
22  
23 box-shaped IRF enables fast NLR analysis, which is critical in a clinical setting such  
24  
25 as ischemic stroke.  
26  
27

28  
29 Time attenuation curve of the tissue and the relative CBV, CBF and TTP maps are  
30  
31 estimated using the calculated AIF with the computed IRF.[10]  
32  
33  
34  
35  
36  
37  
38  
39  
40  
41  
42  
43  
44  
45  
46  
47  
48  
49  
50  
51  
52

### 53 2.3 CNN training 54 55 56 57 58 59 60 61 62 63 64 65

1 In this section we are going to provide an overview on the methods used to train the  
2 artificial neural network model on perfusion CT scans in order to obtain CBV, CBF  
3 and TTP maps as outputs.  
4

5  
6  
7 The filtered registered images are the only input provided to the trained U-Net like  
8 architecture.[13] This particular neural network architecture has been originally  
9 developed for image segmentation: however, it proved to be effective also to solve  
10 other tasks.[14,15] The only proposed change here is the use of average  
11 pooling layers in place of max pool: the use of the standard max-pool layer in our  
12 context is a suboptimal since we do not expect sparse features to be extracted. In  
13 our case, we aim at using it for perfusion map inference: instead of using standard  
14 cross entropy loss, or dice score/focal loss, which are typical for training  
15 segmentation tasks, we minimize the mean squared error loss (MSE), which is  
16 compatible to the desired ground truth output. No additional information (like the AIF)  
17 was provided to the CNN: all the information is implicitly extracted or inferred from  
18 the registered CT scans.  
19  
20  
21  
22  
23  
24  
25  
26  
27  
28  
29  
30  
31  
32  
33  
34  
35

36 The CT scans are processed as a 3D tensor, where the third dimension is  
37 represented by the time scale. Hence, depending on the chosen time granularity, the  
38 number of input channels changes accordingly.  
39  
40  
41  
42  
43

44 The CNN structure is displayed in figure 1.  
45  
46  
47  
48  
49  
50  
51  
52  
53  
54  
55  
56  
57  
58  
59  
60  
61  
62  
63  
64  
65



1  
2  
3  
4  
5  
6  
7  
8  
9  
10  
11  
12  
13  
14  
15  
16  
17  
18  
19  
20  
21  
22  
23  
24  
25  
26  
27  
28  
29  
30  
31  
32  
33  
34  
35  
36  
37  
38  
39  
40  
41  
42  
43  
44  
45  
46  
47  
48  
49  
50  
51  
52  
53  
54  
55  
56  
57  
58  
59  
60  
61  
62  
63  
64  
65

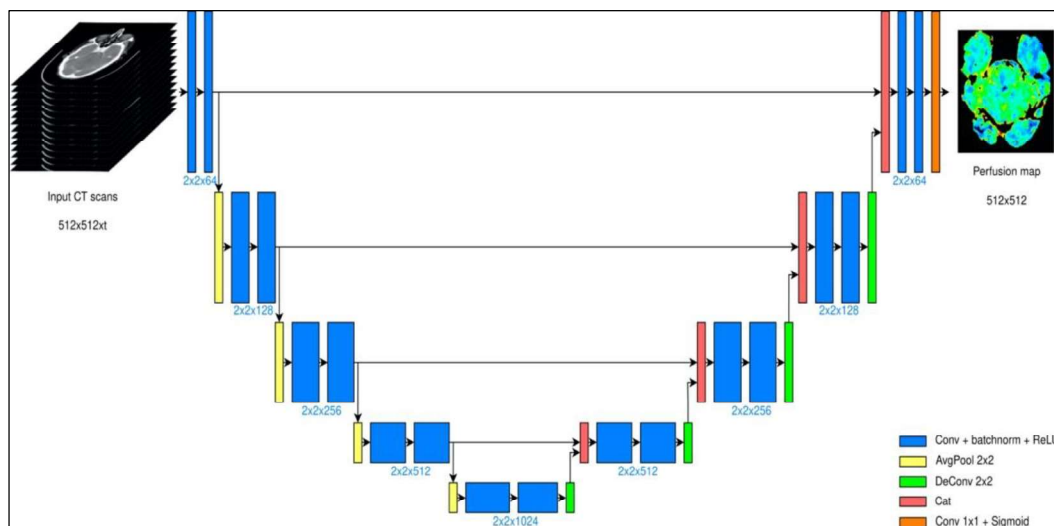


Figure 1. U-Net architecture deployed. The model takes scans of size 512x512, acquired in  $t$  different time instants. The bottleneck layer is placed after four encoding stages, and the output is a 512x512 map

The output of the model is a 512x512 map (figure 2), where all the pixel values are normalized in the range [0; 1]. The entire model has been trained using SGD optimization strategy with learning rate decay policy self-tuned according to the performance on the validation set.

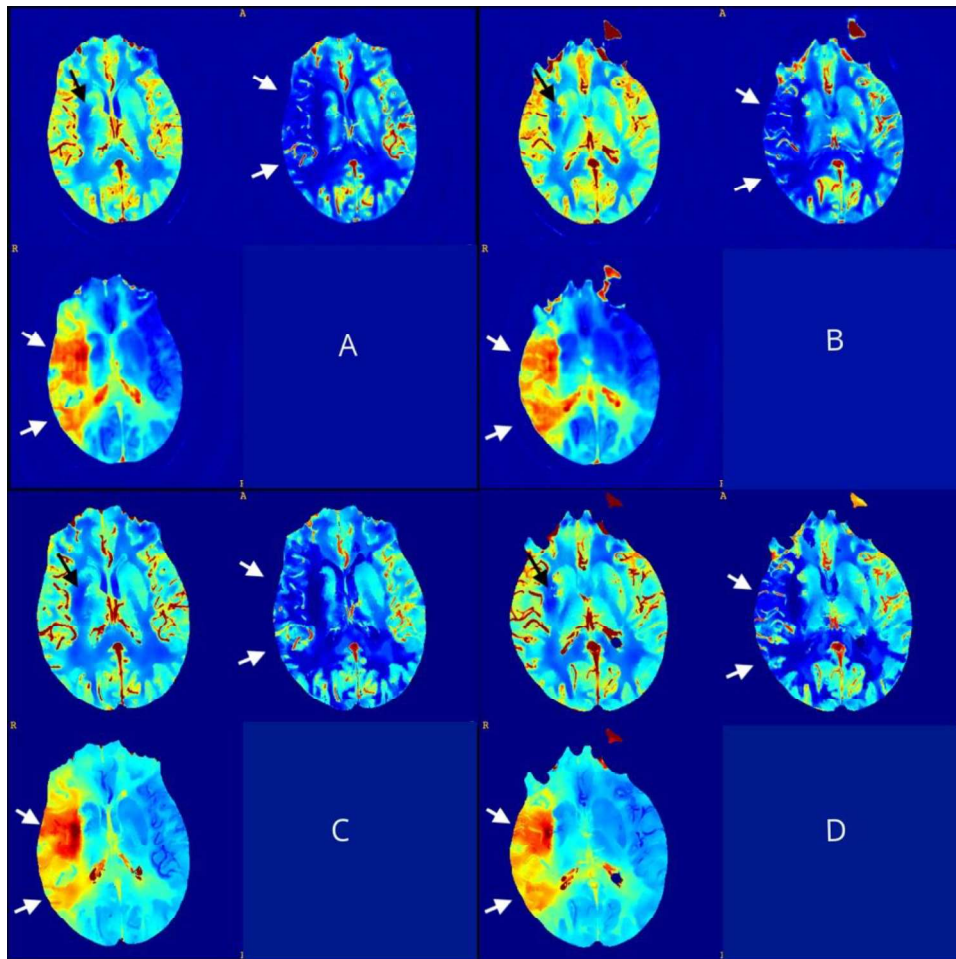


Figure 2. (A, B) CNN outputs maps from a validation set (CBV, CBF and TTP); (C, D) matching sections of GT maps. There is a small infarct core displayed in the CBV map at the right basal ganglia (black arrows) and an extended penumbra showed in the CBF and TTP maps across right middle cerebral artery territories (white arrows).

### 2.3 CNN Validation

Validation is carried out through manual segmentation of the infarct core (CBV) and penumbra (CBF, TTP) on 15 sets of CNN-parametric maps by two expert

radiologists using ITK-SNAP opensource software.[16] Segmentation is carried out section-wise following the axial direction.

To avoid bias induced from repetitive evaluation of the same patient, GT-maps segmentation is sorted out the same way by a third Radiologist.

An example of core segmentation on both CNN and GT maps is displayed in figure 3.

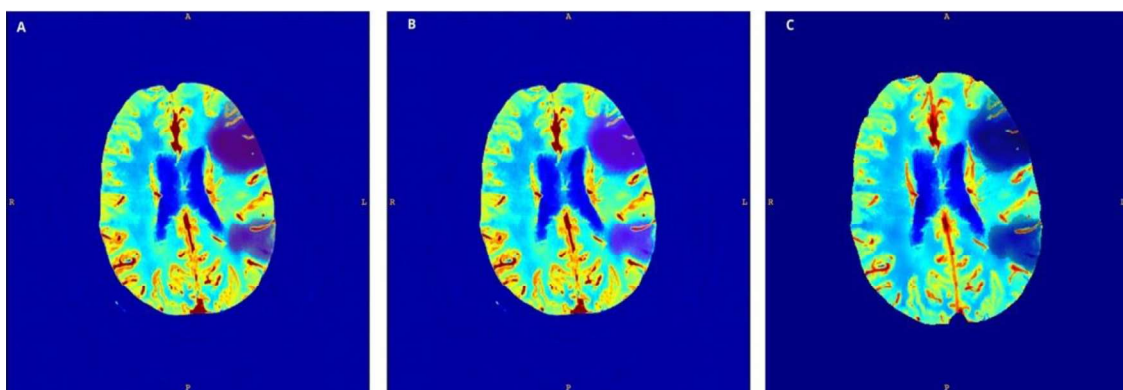


Figure 3. core segmented on CNN CBV map by rater 1 (A) and rater 2 (B); core segmented on GT map (C)

The CNN segmented volumes from both raters were matched with the GT to assess overlapping regions by calculating the Dice Similarity Coefficient (DSC). DSC > 0.70 was considered as good-matching.

DSC were also calculated matching CNN segmentations from different raters to evaluate inter-rater concordance.

Pearson correlation coefficient ( $r$ ) was used to assess the relationship between the lesion volume on GT and CNN maps. Statistical analysis was performed using the 3D-convert toolbox from ITK-SNAP and SPSS software.

### 3. Results

3 out of 15 CTP datasets used as CNN validation exhibited normal perfusion parameters on both GT and CNN-parametric maps and resulted negative for vessel occlusion on CT Angiography (CTA). Normal perfusion maps were excluded from DSC analysis to avoid overestimation of the segmentations comparison results. Segmented core (CBV) and hypo-perfused regions (CBF/TTP) volumes of the remaining patients are shown in figure 4 and 5; 3 out of 12 patients presented with only penumbra territories without ischemic cores.

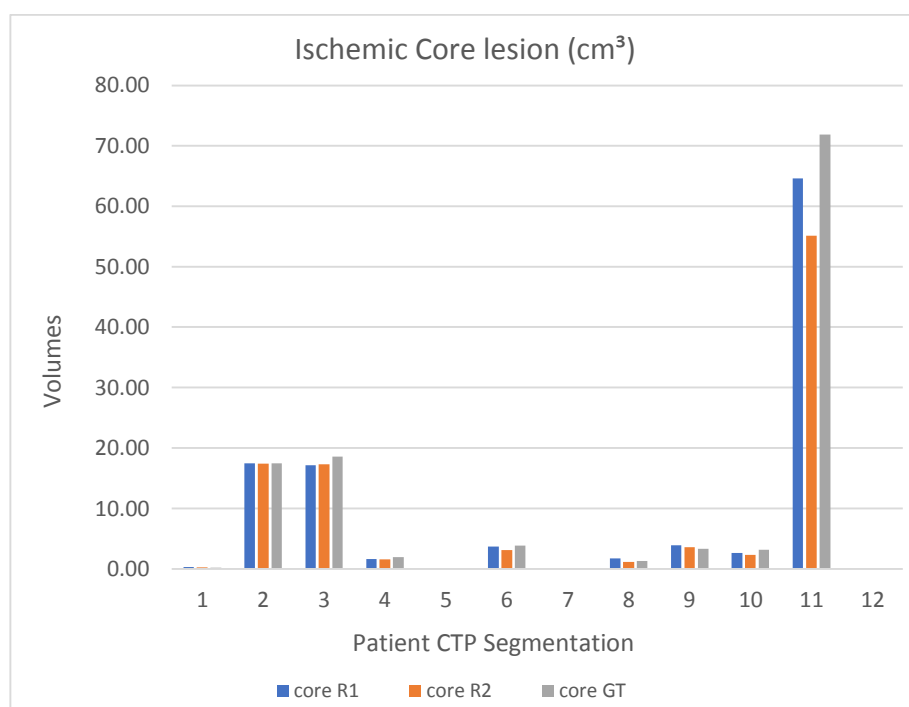


Figure 4. Test sample Ischemic Core segmentation volumes from Rater1 (R1), Rater2 (R2) and GT

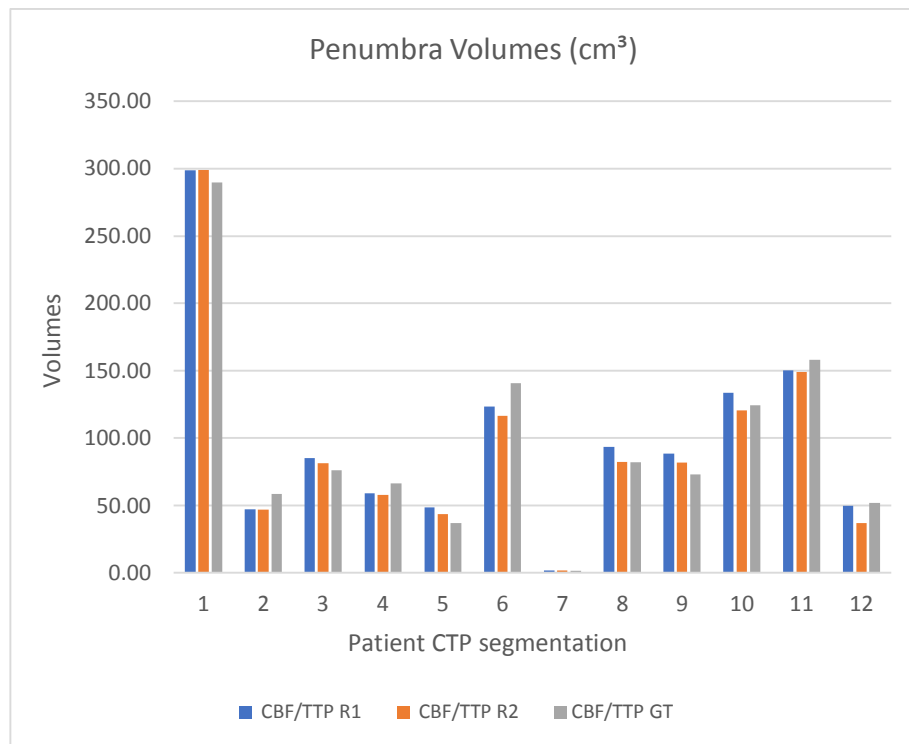


Figure 5. Test sample CBF/TTP segmentation volumes from Rater1 (R1), Rater2 (R2) and GT

Mean DSC for all CBV lesions and CBF/TTP lesions is > 0.70 (Rater1 DSC-CBV 0.82 range 0.71-0.95; Rater2 DSC-CBV 0.79 range 0.73-0.88; Rater1 DSC-CBF/TTP 0.85 range 0.65-0.93; Rater2 DSC-CBF/TTP 0.83 range 0.60-0.92). DSC resulting from segmentation matching are presented as mean and standard deviation (SD) in table 1.

We also find a strong positive correlation ( $r= 0.99$ ,  $r= 0.98$  with  $p<0.001$ ) between CBV - CBF/TPP lesion volume on GT and CNN maps for both raters (table 1).

1  
2  
3  
4  
5  
6  
7  
8  
9  
10  
11  
12  
13  
14  
15  
16  
17  
18  
19  
20  
21  
22  
23  
24  
25  
26  
27  
28  
29  
30  
31  
32  
33  
34  
35  
36  
37  
38  
39  
40  
41  
42  
43  
44  
45  
46  
47  
48  
49  
50  
51  
52  
53  
54  
55  
56  
57  
58  
59  
60  
61  
62  
63  
64  
65

Table 1. Average DSC and lesion volumes Pearson correlations

	CBV	CBF/TTP
Rater1/GT (DSC)	0.82 ± 0.07	0.85 ± 0.07
Rater2/GT (DSC)	0.79 ± 0.05	0.83 ± 0.09
Rater1/Rater2 (DSC)	0.85 ± 0.10	0.87 ± 0.06

Rater1/GT Pearson r	0.99	0.98
Rater2/GT Pearson r	0.99	0.99

Table 1. Resulting DSC of CBV and CBF/TTP segmentation expressed as mean and SD; Pearson correlation between CBV-CBF/TTP volumes on GT and CNN maps

## 4. Discussion

The study demonstrates that parametric maps generated by our CNN can compete with a state-of-the-art CTP NLR algorithm, when working on pre-processed images.

There is a high DSC and strong linear correlation found between CNN and GT segmented volumes.

The performance of our CNN in estimating ischemic core and penumbra is comparable to a state-of-the-art CTP NLR algorithm.

### 4.1 AIF selection is redundant

1  
2 To precisely estimate perfusion parameters, the proposed CNN requires only  
3  
4 registered CT scans while deconvolution-based CT and MRI brain perfusion analysis  
5  
6 methods need additional inputs, such as the AIF curve measured in a large feeding  
7  
8 artery.[17] This suggests that our CNN is capable of combining information from  
9  
10 arterial and tissue signals to obtain quantitative estimates for the CBV, CBF and  
11  
12 MTT. Differently, other recent automated CTP analysis methods such as RAPID,[18]  
13  
14 use AIF and the venous output function from a major venous system before  
15  
16 computing perfusion parameters and subsequently estimating ischemic core and  
17  
18 penumbra.[19]  
19  
20  
21  
22  
23  
24  
25  
26  
27  
28  
29  
30  
31  
32  
33  
34  
35

## 36 4.2 Translation to a general population

37  
38  
39  
40

41 Our validation and training CTP datasets are obtained from a population of patients  
42  
43 eligible for reperfusion therapy, with limited or no hypodense lesions on non-contrast  
44  
45 CT.  
46  
47

48 Such a population was targeted to simulate the clinical setting where CTP is a key  
49  
50 parameter for clinical decisions: when time of onset is not known, CTP allows to  
51  
52 effectively select patients for treatment, as shown in DAWN and DEFUSE-3  
53  
54 trials.[6,7] Furthermore, our method shows accurate performance in patients with no  
55  
56 vessel occlusion on CTA and normal CTP parameters on GT maps, therefore  
57  
58  
59  
60  
61  
62  
63  
64  
65



1 suggesting that our CNN approach should yield reliable results even within the  
2 general population. In order to confirm this hypothesis, though, validation on a wider  
3 sample of CTP data is needed. Moreover, hypodense lesions may mark ischemic  
4 core on CTP; this introduces additional information that may easily be exploited by  
5 CNNs without estimating the tissue-curve offset, as required, instead, by  
6 deconvolution-based algorithms.  
7  
8  
9  
10  
11  
12  
13  
14  
15  
16  
17  
18

### 19 4.3 Limitations

20 Our CNN was tested on a high dose/SNR dataset with limited axial coverage, thus  
21 an application to noisier datasets is required for a complete comparison with state-of-  
22 the-art techniques. Moreover, the CNN should be re-trained using the latest  
23 protocols, with extended axial coverage, from different scanners in order to confirm  
24 our results while working on different environments.  
25  
26  
27  
28  
29  
30  
31  
32  
33  
34  
35  
36  
37  
38  
39  
40  
41

### 42 4.4 Applications and future developments

43 Considering the apparently similar performance of CNNs and deconvolution-based  
44 algorithms, one might ask why the former approach might be preferable. Although  
45 machine learning algorithms have largely proven to overcome conventional image  
46 processing algorithms in practically every field, applications to CTP imaging are still  
47 limited (segmentation,[20–22] noise reduction,[22–24] novelty detection,[23,25]  
48 radiation dose reduction[23]). In particular, up until now generation of synthetic maps  
49  
50  
51  
52  
53  
54  
55  
56  
57  
58  
59  
60  
61  
62  
63  
64  
65

1 has been done only with MRI DSC perfusion by Ho et al. and Meier et al.[26,27]  
2 Meier et al obtained results similar to ours: they compared the performance of a  
3 commercial FDA-approved perfusion software and a CNN not only to generate T-  
4 Max MRI perfusion maps, but also to identify selection criteria for reperfusion  
5 therapies. They concluded that CNN-based approaches may lead to a greater  
6 standardization, faster analysis pipeline and increased robustness.[26] Ho et al.,  
7 instead, estimated voxel-wise MRI perfusion parameters using a deep learning  
8 approach exploiting the concentration time curve and AIF as inputs.[27] Their  
9 approach, however, proved to be time consuming and thus not ideal for clinical  
10 practice.  
11  
12  
13  
14  
15  
16  
17  
18  
19  
20  
21  
22  
23

24 In this preliminary work, pre-processed images were used as input. Further  
25 developments include processing of raw CT acquisitions directly: as demonstrated  
26 by novel deep learning models capable of recovering high quality CT images from  
27 low dose CT scans of perfusion protocols,[24] a certain amount of information is  
28 redundant in CTP images, and currently neural-network-based algorithms probably  
29 represent the most effective way to extract it.  
30  
31  
32  
33  
34  
35  
36  
37  
38

39 Moreover, ischemic core estimate on CNN-derived maps could be compared with  
40 more sensitive gold standards such as MRI diffusion imaging, to obtain further  
41 information on how our method performs in clinical environment.  
42  
43  
44  
45  
46  
47  
48  
49  
50  
51  
52  
53  
54  
55  
56

## 57 Conclusions

58  
59  
60  
61  
62  
63  
64  
65

1 The proposed CNN generated informative perfusion maps of patients with AIS, fairly  
2 approximating perfusion mismatch in brain tissues. Our model can fairly compete  
3 with state-of-the-art perfusion analysis methods in estimating CBF, CBV and TTP.  
4 Moreover, the growing potential of machine learning-based methods of perfusion  
5 analysis can lead to new improved standards in terms of acquisition protocols and  
6 deployed radiation dose.  
7  
8  
9  
10  
11  
12  
13  
14  
15  
16  
17  
18  
19  
20  
21

## 22 Disclosure of interest

23  
24 The authors declare that they have no competing interest.  
25  
26  
27  
28

## 29 Acknowledgements

30 This project was supported by the European Union's Horizon 2020 research and  
31 innovation programme under grant agreement No 825111, DeepHealth Project.  
32  
33  
34

35 Giacomo Vaudano MD, Andrea Boghi MD from the Neuroradiology Department of  
36 San Giovanni Bosco Hospital (Turin) and Simona Veglia MD from the Radiology  
37 Department of Molinette Hospital (Turin) provided help gathering the training dataset.  
38  
39  
40  
41  
42  
43  
44  
45  
46  
47  
48  
49  
50  
51  
52  
53  
54  
55  
56  
57  
58  
59  
60  
61  
62  
63  
64  
65

## References

- 1  
2  
3  
4  
5  
6  
7 [1] Donahue J, Wintermark M. Perfusion CT and acute stroke imaging: Foundations,  
8 applications, and literature review. *Journal of Neuroradiology* 2015.  
9  
10 <https://doi.org/10.1016/j.neurad.2014.11.003>.  
11  
12  
13  
14
- 15 [2] Wannamaker R, Guinand T, Menon BK, Demchuk A, Goyal M, Frei D, et al. Computed  
16 tomographic perfusion predicts poor outcomes in a randomized trial of endovascular  
17 therapy. *Stroke*, 2018. <https://doi.org/10.1161/STROKEAHA.117.019806>.  
18  
19  
20  
21  
22
- 23 [3] Konstas AA, Goldmakher G v., Lee TY, Lev MH. Theoretic basis and technical  
24 implementations of CT perfusion in acute ischemic stroke, part 1: Theoretic basis.  
25 *American Journal of Neuroradiology* 2009. <https://doi.org/10.3174/ajnr.A1487>.  
26  
27  
28  
29
- 30 [4] Konstas AA, Goldmakher G v., Lee TY, Lev MH. Theoretic basis and technical  
31 implementations of CT perfusion in acute ischemic stroke, Part 2: Technical  
32 implementations. *American Journal of Neuroradiology* 2009.  
33  
34  
35  
36  
37  
38 <https://doi.org/10.3174/ajnr.A1492>.  
39  
40
- 41 [5] Campbell BCV, Christensen S, Levi CR, Desmond PM, Donnan GA, Davis SM, et al.  
42 Cerebral blood flow is the optimal CT perfusion parameter for assessing infarct core.  
43 *Stroke* 2011. <https://doi.org/10.1161/STROKEAHA.111.618355>.  
44  
45  
46  
47
- 48 [6] Nogueira RG, Jadhav AP, Haussen DC, Bonafe A, Budzik RF, Bhuva P, et al.  
49 Thrombectomy 6 to 24 hours after stroke with a mismatch between deficit and  
50 infarct. *New England Journal of Medicine* 2018.  
51  
52  
53  
54  
55  
56 <https://doi.org/10.1056/NEJMoa1706442>.  
57  
58  
59  
60  
61  
62  
63  
64  
65

- 1  
2  
3  
4  
5  
6  
7  
8  
9  
10  
11  
12  
13  
14  
15  
16  
17  
18  
19  
20  
21  
22  
23  
24  
25  
26  
27  
28  
29  
30  
31  
32  
33  
34  
35  
36  
37  
38  
39  
40  
41  
42  
43  
44  
45  
46  
47  
48  
49  
50  
51  
52  
53  
54  
55  
56  
57  
58  
59  
60  
61  
62  
63  
64  
65
- [7] Albers GW, Marks MP, Kemp S, Christensen S, Tsai JP, Ortega-Gutierrez S, et al. Thrombectomy for stroke at 6 to 16 hours with selection by perfusion imaging. *New England Journal of Medicine* 2018. <https://doi.org/10.1056/NEJMoa1713973>.
- [8] Kudo K, Sasaki M, Yamada K, Momoshima S, Utsunomiya H, Shirato H, et al. Differences in CT perfusion maps generated by different commercial software: Quantitative analysis by using identical source data of acute stroke patients. *Radiology* 2010. <https://doi.org/10.1148/radiol.254082000>.
- [9] Barber PA, Demchuk AM, Zhang J, Buchan AM. Validity and reliability of a quantitative computed tomography score in predicting outcome of hyperacute stroke before thrombolytic therapy. *Lancet* 2000. [https://doi.org/10.1016/S0140-6736\(00\)02237-6](https://doi.org/10.1016/S0140-6736(00)02237-6).
- [10] Bennink E, Oosterbroek J, Kudo K, Viergever MA, Velthuis BK, de Jong HWAM. Fast nonlinear regression method for CT brain perfusion analysis. *Journal of Medical Imaging* 2016. <https://doi.org/10.1117/1.jmi.3.2.026003>.
- [11] Klein S, Staring M, Murphy K, Viergever MA, Pluim JPW. Elastix: A toolbox for intensity-based medical image registration. *IEEE Transactions on Medical Imaging* 2010. <https://doi.org/10.1109/TMI.2009.2035616>.
- [12] Tomasi C, Manduchi R. Bilateral filtering for gray and color images. *Proceedings of the IEEE International Conference on Computer Vision*, 1998. <https://doi.org/10.1109/iccv.1998.710815>.
- [13] Ronneberger O, Fischer P, Brox T. U-net: Convolutional networks for biomedical image segmentation. *Lecture Notes in Computer Science (including subseries Lecture Notes in Artificial Intelligence and Lecture Notes in Bioinformatics)*, 2015. [https://doi.org/10.1007/978-3-319-24574-4\\_28](https://doi.org/10.1007/978-3-319-24574-4_28).

- 1  
2  
3  
4  
5  
6  
7  
8  
9  
10  
11  
12  
13  
14  
15  
16  
17  
18  
19  
20  
21  
22  
23  
24  
25  
26  
27  
28  
29  
30  
31  
32  
33  
34  
35  
36  
37  
38  
39  
40  
41  
42  
43  
44  
45  
46  
47  
48  
49  
50  
51  
52  
53  
54  
55  
56  
57  
58  
59  
60  
61  
62  
63  
64  
65
- [14] Falk T, Mai D, Bensch R, Çiçek Ö, Abdulkadir A, Marrakchi Y, et al. U-Net: deep learning for cell counting, detection, and morphometry. *Nature Methods* 2019. <https://doi.org/10.1038/s41592-018-0261-2>.
- [15] Chen S, Qin A, Zhou D, Yan D. Technical Note: U-net-generated synthetic CT images for magnetic resonance imaging-only prostate intensity-modulated radiation therapy treatment planning. *Medical Physics* 2018. <https://doi.org/10.1002/mp.13247>.
- [16] Yushkevich PA, Piven J, Hazlett HC, Smith RG, Ho S, Gee JC, et al. User-guided 3D active contour segmentation of anatomical structures: Significantly improved efficiency and reliability. *NeuroImage* 2006. <https://doi.org/10.1016/j.neuroimage.2006.01.015>.
- [17] Fieselmann A, Kowarschik M, Ganguly A, Hornegger J, Fahrig R. Detailed Deconvolution theory and deduction. *International Journal of Biomedical Imaging* 2011. <https://doi.org/10.1155/2011/467563>.
- [18] Campbell BCV, Yassi N, Ma H, Sharma G, Salinas S, Churilov L, et al. Imaging selection in ischemic stroke: Feasibility of automated CT-perfusion analysis. *International Journal of Stroke* 2015. <https://doi.org/10.1111/ijvs.12381>.
- [19] Laughlin BB, Chan A, Tai WA, Moftakhar P. RAPID Automated CT Perfusion in Clinical Practice. *Neuroimaging* 2019.
- [20] Clèrigues A, Valverde S, Bernal J, Freixenet J, Oliver A, Lladó X. Acute ischemic stroke lesion core segmentation in CT perfusion images using fully convolutional neural networks. *Computers in Biology and Medicine* 2019. <https://doi.org/10.1016/j.combiomed.2019.103487>.
- [21] Zhou X, Takayama R, Wang S, Zhou X, Hara T, Fujita H. Automated segmentation of 3D anatomical structures on CT images by using a deep convolutional network based

on end-to-end learning approach. Medical Imaging 2017: Image Processing, 2017.

<https://doi.org/10.1117/12.2254201>.

[22] Kloenne M, Niehaus S, Lampe L, Merola A, Reinelt J, Roeder I, et al. Domain-specific cues improve robustness of deep learning-based segmentation of CT volumes. Scientific Reports 2020. <https://doi.org/10.1038/s41598-020-67544-y>.

[23] Chen H, Zhang Y, Kalra MK, Lin F, Chen Y, Liao P, et al. Low-Dose CT with a residual encoder-decoder convolutional neural network. IEEE Transactions on Medical Imaging 2017. <https://doi.org/10.1109/TMI.2017.2715284>.

[24] Xiao Y, Liu P, Liang Y, Stolte S, Sanelli P, Gupta A, et al. STIR-net: Deep spatial-temporal image restoration net for radiation reduction in CT perfusion. Frontiers in Neurology 2019. <https://doi.org/10.3389/fneur.2019.00647>.

[25] Zhang H, Chen Y, Song Y, Xiong Z, Yang Y, Jonathan Wu QM. Automatic Kidney Lesion Detection for CT Images Using Morphological Cascade Convolutional Neural Networks. IEEE Access 2019. <https://doi.org/10.1109/ACCESS.2019.2924207>.

[26] Meier R, Lux P, Med B, Jung S, Fischer U, Gralla J, et al. Neural Network-derived Perfusion Maps for the Assessment of Lesions in Patients with Acute Ischemic Stroke. Radiology: Artificial Intelligence 2019. <https://doi.org/10.1148/ryai.2019190019>.

[27] Ho KC, Scalzo F, Sarma K v., El-Saden S, Arnold CW. A temporal deep learning approach for MR perfusion parameter estimation in stroke. Proceedings - International Conference on Pattern Recognition, 2016. <https://doi.org/10.1109/ICPR.2016.7899819>.

1  
2  
3  
4  
5  
6  
7  
8  
9  
10  
11  
12  
13  
14  
15  
16  
17  
18  
19  
20  
21  
22  
23  
24  
25  
26  
27  
28  
29  
30  
31  
32  
33  
34  
35  
36  
37  
38  
39  
40  
41  
42  
43  
44  
45  
46  
47  
48  
49  
50  
51  
52  
53  
54  
55  
56  
57  
58  
59  
60  
61  
62  
63  
64  
65

Figure

